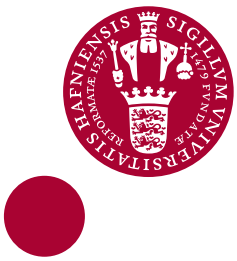

# A New Negative Allosteric Modulator AP14145 for the Study of Small Conductance Calcium-Activated Potassium Channels

Simo Vicens, Rafel; Kirchhoff, Jeppe Egedal; Dolce , Bernardo ; Abildgaard, Lea; Speerschneider, Tobias; Sørensen, Ulrik Svane; Grunnet, Morten; Diness, Jonas Goldin; Bentzen, Bo Hjorth

*Published in:*
British Journal of Pharmacology

*DOI:*
10.1111/bph.14043

*Publication date:*
2017

*Document version*
Peer reviewed version

# A New Negative Allosteric Modulator AP14145 for the Study of Small Conductance Calcium-Activated Potassium Channels

**Running title: Novel $K_{Ca}2$ Channel Inhibitor**

Rafel Simó-Vicens[1,2], Jeppe E. Kirchhoff[2], Bernardo Dolce[3], Lea Abildgaard Jensen[2], Tobias Speerschneider[2], Ulrik S. Sørensen[2], Morten Grunnet[2], Jonas G. Diness[2], Bo H. Bentzen[1,2]

[1]*Biomedical Institute, University of Copenhagen, Blegdamsvej 3B, DK-2200, Copenhagen, Denmark*

[2]*Acesion Pharma, Ole Maaløes Vej 3, DK-2200, Copenhagen, Denmark.*

[3]*Department of Experimental Pharmacology and Toxicology, University Medical Center Hamburg-Eppendorf, Germany & DZHK (German Center for Cardiovascular Research), partner site Hamburg/Kiel/Lübeck, Hamburg*

Corresponding author: Bo H. Bentzen, bobe@sund.ku.dk, Blegdamsvej 3B, DK-2200, Copenhagen, Denmark

**Abbreviations**:

AERP: atrial effective refractory period

AF: atrial fibrillation

$K_{Ca}1.1$ big conductance calcium-activated potassium channel

$K_{Ca}2$: small conductance calcium-activated potassium channel

$K_{Ca}3.1$: intermediate conductance calcium-activated potassium channel

PEG: polyethylene glycol

WT: wild type

## Abstract

**Background and purpose:** Small conductance $Ca^{2+}$-activated $K^+$ ($K_{Ca}2$) channels represent a promising atrial-selective target for treatment of atrial fibrillation (AF). Here, we establish the mechanism of $K_{Ca}2$ inhibition by the new compound AP14145.

**Experimental approach:** Using site directed mutagenesis binding determinants for AP14145 inhibition were explored. AP14145 selectivity and mechanism of action were investigated by patch clamp recordings of heterologously expressed $K_{Ca}2$ channels. The biological efficacy of AP14145 was assessed by measuring atrial effective refractory period (AERP) prolongation in anaesthetised rats and a beam walk test was performed in mice to determine acute CNS related effects of the drug.

**Key results:** AP14145 was found to be an equipotent negative allosteric modulator of $K_{Ca}2.2$ and $K_{Ca}2.3$ channels ($IC_{50}$ = 1.1 ± 0.3 μM $L^{-1}$). The presence of AP14145 (10 μM $L^{-1}$) increased the $EC_{50}$ of $Ca^{2+}$ on $K_{Ca}2.3$ from 0.36 ± 0.02 μM $L^{-1}$ to 1.2 ± 0.1 μM $L^{-1}$. The inhibitory effect strongly depended on two amino acids, S508 and A533. AP14145 concentration-dependently prolonged AERP in rats. Moreover, AP14145 (10 mg $kg^{-1}$) did not trigger any apparent CNS effects in mice.

**Conclusion and implications:** AP14145 is a negative allosteric modulator of $K_{Ca}2.2$ and $K_{Ca}2.3$ that shifts the calcium dependence of channel activation, an effect strongly dependent on two identified amino acids. AP14145 prolongs AERP in rats and does not trigger any acute CNS effects in mice. The understanding of how $K_{Ca}2$ inhibition is accomplished at the molecular level will help future development of drugs targeting $K_{Ca}2$ channels.

## Introduction

Small conductance calcium-activated potassium channels ($K_{Ca}2.1$, $K_{Ca}2.2$ and $K_{Ca}2.3$ channels) are widely distributed in humans (Chen et al., 2004), where they serve important roles such as contributing to the afterhyperpolarization in neurons (Pedarzani et al., 2005), the endothelium-derived hyperpolarization (Milkau et al., 2010) or the late repolarization phase in cardiomyocytes (Li et al., 2009). These channels are constitutively associated to calmodulin, which binds intracellular calcium and activates $K_{Ca}2$ (Adelman, 2016). Since cloning of the channels 20 years ago (Köhler et al., 1996), they have piqued the interest of pharmacologists in different therapeutic areas. Although at the beginning most of the efforts were focused on the CNS and the treatment of neurodegenerative and psychiatric diseases (Lam et al., 2013), the therapeutic potential of $K_{Ca}2$ channels rapidly spread to other areas (Wulff et al., 2007). Currently, one of the most promising therapeutic opportunities for $K_{Ca}2$ channel modulation seems to be in cardiovascular diseases, more specifically in atrial fibrillation (AF).

AF is the most common type of cardiac arrhythmia and it is considered one of the largest public health problems in developed countries (Zoni-Berisso et al., 2014). The disease is characterized by rapid uncoordinated activation of the atria, resulting in reduced ventricular filling and blood stasis in atria, which predisposes to heart failure and thromboembolic stroke (Nattel, 2002). Unfortunately, current rhythm therapy is only moderately effective and may trigger serious non cardiac as well as ventricular adverse effects (Waks and Zimetbaum, 2017).

$K_{Ca}2$ channels are considered a promising new target for AF treatment for several reasons. First, the functional role of $K_{Ca}2.2$ and $K_{Ca}2.3$ channels appears to be greater in the atria as compared to ventricles which may help avoiding undesired ventricular adverse effects (Diness et al., 2015). Second, $K_{Ca}2$ channel inhibition prolongs the atrial effective refractory period (AERP, Diness *et al.*, 2010), a pharmacological strategy that has successfully been used in the development of other class III antiarrhythmic drugs (Schmitt et al., 2014). Furthermore, common variants of the genes that encode $K_{Ca}2.2$ and $K_{Ca}2.3$ have been associated with atrial fibrillation (Ellinor et al., 2010; Christophersen et al., 2017).

The first described negative allosteric modulator was NS8593 (Fig 1), a chiral 2-aminobenzimidazole derivative able to inhibit $K_{Ca}2$ channels at nanomolar

concentrations with no subtype selectivity (Strøbæk et al., 2006; Sørensen et al., 2008). The negative modulation of NS8593 relies in the compound's ability to increase $Ca^{2+}$ $EC_{50}$ for $K_{Ca}2$ activation and its binding site has been found to be in the inner pore vestibule of the channel (Jenkins et al., 2011).

$K_{Ca}2$ channels are widely expressed in the CNS (Stocker and Pedarzani, 2000) and therefore one of the challenges encountered during the development of compounds targeting peripheral $K_{Ca}2$ is potential CNS mediated adverse effects (Habermann, 1984). It is thus important to develop compounds with reduced blood brain barrier penetrance in order to avoid possible adverse effects. In this work, we present a novel $K_{Ca}2$ negative allosteric modulator, AP14145 (Fig 1), a structurally close analogue of NS8593 designed to inhibit specifically peripheral $K_{Ca}2$ channels by preventing its entry in the CNS. In contrast to NS8593, it does not appear to have any immediate CNS effects when dosed to rodents and therefore represents a new and improved tool compound for studying $K_{Ca}2$ channel inhibition in rodents *in vivo*.

## Methods

### *Molecular biology*

$rK_{Ca}2.3$ WT (wild type) and $rK_{Ca}2.3$ S508T A533V were inserted in pXOON plasmids. The $rK_{Ca}2.3$ NS8593 insensitive mutant was obtained by introducing the double point mutation to the WT $rK_{Ca}2.3$ with the oligonucleotides CCATAGCCAATggtAAGGAACGTGATG for S508T and CATCATGGGTgtaGGCTGCACTGCCCTC for A533V, using PfuUltra II Fusion polymerase (Agilent, USA) and T4 ligase (New England Biolabs, USA). Note that S508 and A533 on the $rK_{Ca}2.3$ are the equivalent positions of S507 and A532 on the $hK_{Ca}2.3$ channel. Competent *E. coli* were transformed using an aliquot of the mutagenesis product by thermic shock and the plasmid DNA was purified using standard methods. The $hK_{Ca}3.1$ T250S V275A mutant was kindly donated by Dorte Strøbæk. All constructs were verified by sequencing.

### *Cell culture and cell preparation*

To study the effect of AP14145 on the $hK_{Ca}1.1$ and $hK_{Ca}2.x$ channels we used four different stable HEK293 cell lines expressing $hK_{Ca}1.1$, $hK_{Ca}2.1$, $hK_{Ca}2.2$ or $hK_{Ca}2.3$

channels obtained from NeuroSearch A/S (Ballerup, Denmark). The cell lines were established as described in Strøbæk et al., 2004. For the identification of the binding determinants of AP14145, wild-type HEK293 cells were transiently co-transfected with $rK_{Ca}2.3$ WT, $rK_{Ca}2.3$ S508T A533V, $hK_{Ca}3.1$ WT or $hK_{Ca}3.1$ T250S V275A and 0.1 µg of eGFP plasmid DNA using standard Lipofectamine™ (Thermo Fisher, USA) protocols. Between one or two days after the transfection, patch clamp experiments were conducted. The cells were cultured in Dulbecco's modified Eagle's medium (DMEM1965, Thermo Fisher, USA) supplemented with 26.2 mM $L^{-1}$ $NaHCO_3$, 25 mM $L^{-1}$ HEPES, 10 ml $L^{-1}$ Glutamax (Gibco, USA), 10 % foetal bovine serum (Biowest, France) and 100 U $ml^{-1}$ of penicillin/streptomycin (Sigma, Germany). In the case of the stable cell lines, 100 µg $ml^{-1}$ geneticin (Gibco, USA) were added to the medium. On the day of the experiment, cells were detached from the flask using 1 ml of Detachin™ (Amsbio, United Kingdom). After being washed with free calcium and magnesium PBS the cells were plated on 0.5 mm Ø coverslips. In the case of inside-out patch clamp, the coverslips were treated overnight at 37ºC with 50 mg $ml^{-1}$ poly-L-lysine (Sigma, Germany) to get firmer cell attachment.

*Solutions and drugs*

$K_{Ca}2$ and $K_{Ca}3.1$ patch-clamp experiments were conducted using symmetrical $K^+$ solutions. The extracellular solution contained 0.1 mM $L^{-1}$ $CaCl_2$, 3 mM $L^{-1}$ $MgCl_2$, 154 mM $L^{-1}$ KCl, 10 mM $L^{-1}$ HEPES and 10 mM $L^{-1}$ glucose (pH = 7.4 and 285 - 295 mOsm). The intracellular solution contained 8.106 mM $L^{-1}$ $CaCl_2$ (final free $Ca^{2+}$ concentration of 400 nM $L^{-1}$), 1.167 mM $L^{-1}$ $MgCl_2$, 10 mM $L^{-1}$ EGTA, 154 mM $L^{-1}$ KCl, 10 mM $L^{-1}$ HEPES, 31.25/10 mM $L^{-1}$ KOH/EGTA and 15 mM $L^{-1}$ KOH (pH = 7.2). In addition, to study the activation of the channel with or without the presence of AP14145 we used a range of intracellular solutions containing different free $Ca^{2+}$ concentrations (0.01 - 30 µM $L^{-1}$). The composition of these intracellular solutions was determined as described in Strobaek *et al.*, 2006.

For $K_{Ca}1.1$ the extracellular solution contained 2 mM $L^{-1}$ $CaCl_2$, 1 mM $L^{-1}$ $MgCl_2$, 145 mM $L^{-1}$ NaCl, 4 mM $L^{-1}$ KCl, 10 mM $L^{-1}$ HEPES and 10 mM $L^{-1}$ glucose (pH = 7.4 and 285 - 295 mOsm). The intracellular solution contained 5.374 mM $L^{-1}$ $CaCl_2$ (final free $Ca^{2+}$ concentration of 100 nM $L^{-1}$), 1.75 mM $L^{-1}$ $MgCl_2$, 120 mM $L^{-1}$ KCl, 10 mM $L^{-1}$ HEPES, 31.25/10 mM $L^{-1}$ KOH/EGTA (pH = 7.2).

The osmolarity of the intracellular solutions was adjusted using sucrose (Sigma, Germany) to match the extracellular solutions.

AP14145 (*N*-(2-{[(1*R*)$^{-1}$-[3-(trifluoromethyl)phenyl]ethyl]amino}$^{-1}$*H*$^{-1}$,3-benzodiazol-4-yl)acetamide) was synthetized by Syngene (India) as described in WO 2013104577 A1. For *in vitro* experiments, AP14145 was solubilized in pure DMSO (Sigma-Aldrich, Germany) at 10 mM $L^{-1}$ stock solutions. These stock solutions were stored at -20°C and aliquots were solubilized at the desired concentration on the day of the experiment. For *in vivo* experiments, 5 mg $ml^{-1}$ AP14145 were dissolved in a vehicle consisting of 50% polyethylene glycol (PEG) 400 (Merck, Germany) and 50% sterile saline (PanReac AppliChem, Germany) for infusion and the solution was sterile filtered (Nalgene, Rapid flow 90 mM $L^{-1}$ filter unit, Thermo Scientific, USA) before use. The $K_{Ca}1.1$ selective inhibitor paxilline was purchased from Sigma-Aldrich (Germany).

*Electrophysiology*

Patch clamp recordings were made using a HEKA EPC9 amplifier and the Patchmaster software (HEKA Elektronik, Germany) at room temperature. Patch pipettes were pulled using a horizontal DMZ Universal Puller (Zeitz, Germany) with resistances of 2.5 ± 0.1 MΩ for whole-cell patch clamp and 2.2 ± 0.6 MΩ for inside-out patch clamp. $K_{Ca}2$ and $K_{Ca}3.1$ currents were elicited every 2 seconds using a 200 ms voltage ramps ranging -80 mV to +80 mV from a holding potential of 0 mV. $K_{Ca}1.1$ currents were elicited every 2 seconds using a 200 ms voltage ramps ranging -80 mV to +50 mV from a holding potential of 0 mV. Data were sampled at 10 kHz. Series resistance values were 5.4 ± 0.6 MΩ with 80% of compensation. Two Bessel filters of 10 kHz and 2.9 kHz were used to avoid background noise.

*Plasma Protein Binding*

Plasma protein binding (PPB) was experimentally determined by Syngene International (India) in rat plasma using rapid equilibrium dialysis.

***Ex vivo experiments***

*Ex vivo* and *in vivo* experiments were performed under a license from the Danish Ministry of justice (license No 2013$^{-1}$5-2934/00964) and in accordance with the Danish guidelines for animal experiments according to the European Commission Directive 86/609/EEC. The animals were housed in groups of 2-4 in high-top cages with bedding

(wood shavings) and under constant climatic conditions (22°C) at the Department of Experimental Medicine, University of Copenhagen. The animals were kept at a 12 hour light-dark cycle with ad libitum access to clean water and standard laboratory rodent diet.

*Isolated perfused heart preparation*

Rats express $K_{Ca}2$ channels in the atria, and have previously been used to study the effect of $K_{Ca}2$ inhibition on atrial refractoriness. Male Sprague-Dawley rats (250 - 350 g, 1-3 months old, Janvier Labs, France) were anaesthetized with fentanyl-midazolam mixture, 5 mg $ml^{-1}$ dose 0.3 mL/100 g BW, s.c. A tracheotomy was performed in the ventilated rat. The aorta was cannulated and the heart was excised, and connected to a Langendorff retrograde perfusion setup (Hugo Sachs Elektronik, Harvard Apparatus GmbH, Germany). The heart was retrogradely perfused with Krebs–Henseleit buffer (in mM $L^{-1}$: NaCl 120.0, $NaHCO_3$ 25.0, KCl 4.0, $MgSO_4$ 0.6, $NaH_2PO_4$ 0.6, $CaCl_2$ 2.5, Glucose 11.0, saturated with 95% $O_2$ and 5% $CO_2$, 37°C, pH 7.4) at a constant perfusion pressure of 80 mmHg. The electrical activity of the heart was measured by volume conducted electrocardiograms (ECGs) and the atrial epicardial monophasic action potentials by an electrode on the right atrium. The signal was sampled at 1 kHz (PowerLab systems, ADInstruments, UK) and monitored by using LabChart 7 software (ADInstruments, UK). The hearts were immersed into a temperature-controlled and carbonated bath containing Krebs–Henseleit buffer. A bipolar pacing electrode was placed on the right atria in order to stimulate the heart and measure the AERP, which was defined as the longest S1-S2 interval failing to elicit an action potential. The AERP was measured every five minutes by applying electrical stimulation (2 times rheobase) with a fixed interval of 133 ms (S1 stimulation) and for every $10^{th}$ beat an extra stimulus (S2 stimulation) was applied with 1 ms increments.

Baseline recordings were made for at least 20 minutes and continued until the ECG morphology and AERP recording were stable. After the baseline recording, four 20-minute episodes followed in which, the heart, was perfused with: 1) 1 µM $L^{-1}$ paxilline 2) 3 µM $L^{-1}$ paxilline 3) washout 4) 10 µM $L^{-1}$ AP14145 and AERP measurements were performed every fifth minute. Measurements after 20 minutes of drug perfusion or washout were used for statistical analysis.

***In vivo experiments***

*Closed chest recording of atrial refractoriness in rats*

A total of 18 1-3 months old male Sprague-Dawley rats (Janvier, France) weighing 400-550 g were anesthetized and randomly divided in three groups: one group receiving AP14145 as bolus injections (n=6), a time matched control group receiving vehicle as bolus injections (n=6), and a group receiving AP14145 as a constant-rate infusion (n=6). The rats were anaesthetized with 3 % isofluran/oxygen and an intravenous catheter was placed in the femoral vein for drug injection. Needle ECG electrodes were placed in each limb for ECG recordings (ADinstruments, UK). The temperature of the rats was monitored and kept stable during the experiment with a heating lamp (37 $^{o}$C). A catheter with eight electrodes (Millar Inc., US) was placed in the right atrium of an anaesthetized rat via the jugular vein. Two of the electrodes were used to pace the atrium and six electrodes were used to measure the electrical activity in the atrium. This combination allows measurements of the AERP and the changes in AERP as a consequence of injection of the test compound. Once the experiment was completed, rats were euthanized by a mixture of 200 mg ml$^{-1}$ pentobarbital and 20 mg ml$^{-1}$ lidocaine hydrochloride (Glostrup Apotek, Denmark) i.v. injection. Since the risk of placebo effect and subjective interpretation of the results was inexistent or minimal, no blinding was used.

*Measurement of AERP*

Each experiment lasted for at least 60 minutes and was divided into three 20-minutes episodes. During the entire experiment the ECG was monitored. The AERP was measured by applying electrical stimulation (5 times rheobase) with a fixed interval of 120 ms (S1 stimulation) and for every 10th beat an extra stimulus (S2 stimulation) was applied with 1 ms increments. The AERP was defined as the longest S1-S2 interval failing to elicit an action potential. Between the AERP recordings, the heart remained unpaced. Baseline AERP recordings with no compound present were made every 5th minute for 20 minutes before adding test compound.

*Increasing bolus dosing*

After the baseline recording, two 20-minute episodes followed in which two groups of rats (n=6 each) were injected with increasing doses of AP14145 (2.5 mg kg$^{-1}$ and 5.0 mg kg$^{-1}$) or equivalent volumes of vehicle (50% PEG-400 and 50% saline). The

injection time was 30 seconds. AERP was measured 1, 5, 10 and 15 minutes after the start of each injection.

*Constant rate infusion of AP14145*

After the baseline recording, a third group of rats received a constant rate infusion of 40 mg $kg^{-1}$ $h^{-1}$ AP14145 over 20 minutes followed by a 20-minute post-infusion period. In these animals the AERP was measured every 2 minutes during and after infusion.

*Beam walk test - assessment of motor balance and coordination in mice*

A beam walk test was performed in mice in order to assess CNS exposure of $K_{Ca}2$ inhibitors in vivo. The mouse beam walk test is a validated test for addressing motor function (Brooks and Dunnett, 2009). Three groups of 1-2 months old male NMRI mice (Taconic Biosciences, USA) weighing 23-49 g were used. The mice were randomly assigned to either the vehicle control group, a 10 mg $kg^{-1}$ NS8593 or a 10 mg $kg^{-1}$ AP14145 group. The mice were placed on a 1 meter wooden beam (ø 12 mm) and briefly trained in crossing the beam. After training, a 1 minute baseline recording was initiated and the number of falls and slips were noted. Hereafter the mice were randomly assigned to receive $K_{Ca}2$ inhibitors or vehicle (50% PEG-400 and 50% saline) by i.v. bolus injection in the tail vein. The mouse was observed immediately after injection for any behavioural changes. If any adverse effects occurred, the mouse was euthanized. Otherwise the mice were observed for behavioural changes and challenged with the beam walk 12 minutes post injection. All experiments were documented by video recordings.

*Data analysis*

Data was extracted from PatchMaster and analysed using GraphPad Prism 7.

To calculate the $IC_{50}$ value of AP14145, the measured currents were first normalized. Recorded currents without the presence of the drug were used as baseline and currents recorded at the highest tested concentration of AP14145 (30 µM $L^{-1}$) were used as total inhibition of the channel. Individual $IC_{50}$ values for each experiment were calculated using the equation:

$$Y = Ymin + \frac{(Ymax - Ymin)}{1 + 10^{X - logIC50}}$$

where X is the log of dose of AP14145 and Y is the normalized measured current. In all cases a Hill slope of -1.0 was considered. Individual $IC_{50}$ values were later used to obtain the final $\bar{x}$ ± SEM. $IC_{50}$. The individual $IC_{50}$ values were then used in student's t-tests to determine subtype selectivity.

To calculate the $EC_{50}$ of calcium, the values were normalized using the currents recorded at the lowest calcium concentration (0.01 µM $L^{-1}$) for total inactivation and at the highest calcium concentration (30 µM $L^{-1}$) for maximum activation of the channel. Individual $EC_{50}$ values for each experiment were calculated using the equation:

$$Y = Ymin + \frac{(Ymax - Ymin)}{1 + 10^{(logEC50 - X) \times HillSlope}}$$

where X is the log of dose of calcium and Y is the normalized measured current with variable Hill slope. Individual $EC_{50}$ values were used to determine the final $\bar{x}$ ± SEM $EC_{50}$.

Currents were also normalized to assess and compare the inhibitory effect of 10 µM $L^{-1}$ AP14145 on HEK cells expressing $K_{Ca}1.1$, $K_{Ca}2.1$, $K_{Ca}2.2$, $K_{Ca}2.3$, $K_{Ca}2.3$ S508T A532V, $K_{Ca}3.1$ or $K_{Ca}3.1$ T250S V275A. For each individual cell, 0% current was defined as 0 nA and 100% current was defined as the current recorded in the absence of the compound. The final results are summarized as $\bar{x}$ ± SEM of the individual values.

To quantify and compare the activation and inhibition effects of 10 µM $L^{-1}$ NS309 and 10 µM $L^{-1}$ AP14145 on the $K_{Ca}2.3$ channel, values were normalized for each individual cell. In this case, 0 was defined as 0 nA and currents recorded in the absence of both compounds were defined as 1. These individual values were used to calculate the final $\bar{x}$ ± SEM.

The last ten data points obtained after the application of a new compound or solution and corresponding to the steady state were used to create every single value.

Student's t-test was performed to assess statistical significance of the effect of AP14145. P values < 0.05 were considered significant.

Physicochemical properties of AP14145 and NS8593 were calculated using the Instant JChem (ChemAxon) software.

Perfused rat heart data and closed chest continuous data are summarized using the $\bar{x}$ ± SEM. A one-way ANOVA with Tukey's comparison post-test was used to compare the

effect of paxilline and AP14145 on the isolated rat heart. Multiple t tests with Holm-Sidak's correction for multiple comparisons were used to compare AERP differences between the group of rats that received AP14145 as increasing bolus doses and the time matched control group at matching time points. Multiple t tests with Holm-Sidak's correction for multiple comparisons were used to compare each AERP-value during and after infusion to the mean baseline AERP values. P values < 0.05 were considered significant.

*Nomenclature of Targets and Ligands*

Key protein targets and ligands in this article are hyperlinked to corresponding entries in http://www.guidetopharmacology.org, the common portal for data from the IUPHAR/BPS Guide to PHARMACOLOGY (Southan et al., 2016), and are permanently archived in the Concise Guide to PHARMACOLOGY 2015/16 (Alexander et al., 2015).

## Results

*AP14145 inhibits both $hK_{Ca}2.2$ and $hK_{Ca}2.3$ currents with equal potency*

Using inside-out manual patch clamp we tested AP14145 on both the $hK_{Ca}2.2$ and $hK_{Ca}2.3$ channels. Once the patch was excised, the channels were exposed to the bath's intracellular solution, containing 400 nM $L^{-1}$ free $[Ca^{2+}]$. In symmetrical intra- and extra-cellular $K^+$ solutions, $hK_{Ca}2.3$ currents displayed a characteristic inwardly rectifying current-voltage relationship (Fig 2a). Currents were elicited using voltage ramps from -80 mV to +80 mV applied every 2 seconds. Once the $hK_{Ca}2$ current was stable, up to 8 increasing concentrations of AP14145 between 0.01 - 30 µM $L^{-1}$ were applied and perfused by gravity flow on the patch (Fig 2b). For each concentration the drug was applied until steady state was reached.

AP14145 was able to inhibit both $hK_{Ca}2.2$ and $hK_{Ca}2.3$ in a concentration-dependent fashion (Fig 2b, data not shown for $hK_{Ca}2.2$). The effect started at nanomolar concentrations and total inhibition was reached at 30 µM $L^{-1}$ (Fig 2b). Calculated $IC_{50}$ for AP14145 on both the $hK_{Ca}2.2$ and $hK_{Ca}2.3$ was 1.1 ± 0.3 µM $L^{-1}$ (n = 7 each, Fig 2c), with a fixed Hill slope of -1.0. The drug consequently did not display any subtype selectivity between $hK_{Ca}2.2$ and $hK_{Ca}2.3$.

Additionally, the inhibitory effect of AP14145 was also tested on the $hK_{Ca}1.1$, $hK_{Ca}2.1$ and $hK_{Ca}3.1$ channels using whole cell patch clamp for further selectivity assessment (Fig 3). The application of 10 µM $L^{-1}$ AP14145 inhibited 50 ± 10% of the $hK_{Ca}1.1$ current (n = 6) and 90 ± 4% of the $hK_{Ca}2.1$ current (n = 7). In contrast, $hK_{Ca}3.1$ currents were not significantly affected by the application of 10 µM $L^{-1}$ AP14145 (n = 8).

*AP14145 modifies $hK_{Ca}2.3$ calcium sensitivity*

To establish how AP14145 inhibits the channel, we performed inside out patch clamp recordings to assess the effect of the drug on the calcium sensitivity of the $hK_{Ca}2.3$ channel. Patches were excised from HEK cells stably expressing the $hK_{Ca}2.3$ channel and currents elicited using voltage ramps. We exposed the patches to eight different free $Ca^{2+}$ concentrations and calculated the $EC_{50}$ for calcium activation of the channel in the absence and presence of 10 µM $L^{-1}$ AP14145 (Fig 4a and b). Free calcium concentrations ranged from 0.01 - 30 µM $L^{-1}$ and were perfused using gravity flow. Solutions were applied until steady state was reached.

In the absence of AP14145, $hK_{Ca}2.3$ channels were fully activated at 3 µM $L^{-1}$ of intracellular $Ca^{2+}$ (Fig 4a), but in the presence of 10 µM $L^{-1}$ AP14145, up to 10 µM $L^{-1}$ were needed to reach total activation of the channel (Fig 4b). At a 10 µM $L^{-1}$ concentration, the drug shifted the calcium-activation curve of the $K_{Ca}2.3$ channel to the right (Fig 4c), so higher calcium concentrations were needed to activate the channels. This was also shown by the significantly increased $EC_{50}$ of $Ca^{2+}$ from 0.36 ± 0.02 µM $L^{-1}$ (n = 9) to 1.3 ± 0.2 µM $L^{-1}$ (n = 7). Most prominently, the Hill coefficients were also significantly modified by the presence of AP14145 from 5.2 ± 0.3 to 1.2 ± 0.1 (absence of AP14145 vs. 10 µM $L^{-1}$ AP14145).

*AP14145 reverses the effect of the positive $K_{Ca}2$ gating modulator NS309*

The inhibitory effect of AP14145 was also studied in the presence of a high concentration of the $K_{Ca}2$ positive gating modulator NS309. Patches excised from HEK cells stably expressing the $hK_{Ca}2.3$ channel were exposed to 400 nM $L^{-1}$ free $[Ca^{2+}]$ intracellular solution. After stabilisation of the baseline, 10 µM $L^{-1}$ NS309 were applied on the patch, further activating the channel and increasing $hK_{Ca}2.3$ current by 4 ± 1 fold (n = 7, Fig 5). When steady state was reached, 10 µM $L^{-1}$ AP14145 were added to the bath, in the continued presence of NS309. The application of AP14145 reduced $hK_{Ca}2.3$ current to values close to the control baseline, reversing the positive gating effect of

NS309 (Figure 5). Furthermore, in the presence of 10 µM $L^{-1}$ NS309, total current inhibition by 10 µM $L^{-1}$ AP14145 was significantly diminished from 80 ± 3% (n = 7) to 61 ± 4% (n = 7, Fig 5).

*AP14145 inhibition strongly depends on two amino acids, S508 and A533, located in the inner pore of the channel*

To establish possible molecular determinants of $rK_{Ca}2.3$ inhibition by AP14145 we mutated two amino acids, S508 and A533 (corresponding to S507 and A532 in $hK_{Ca}2.3$), located in the inner pore of the channel and known to confer sensitivity to the negative allosteric modulator of $K_{Ca}2$ channels, NS8593 (Jenkins et al., 2011).

Whole-cell patch clamp experiments were conducted on transiently transfected HEK cells with either the WT $rK_{Ca}2.3$ channel or the $rK_{Ca}2.3$ S508T A533V mutant. The channels were activated by 400 nM $L^{-1}$ free $[Ca^{2+}]$ intracellular solution and currents were elicited using voltage ramps. Again, in symmetrical intra- and extra-cellular $K^+$ solutions, WT $rK_{Ca}2.3$ currents displayed a characteristic inwardly rectifying current-voltage relationship (Fig 6a). In contrast to the WT $rK_{Ca}2.3$ channel, the maximum current normalized to cell capacitance of the mutant $rK_{Ca}2.3$ was significantly reduced (WT: 650 ± 96 pA/pF vs. mutant: 87 ± 23 pA/pF, n = 7 each, Fig 6b). Rectification, determined as the ratio of the current amplitude at – 80 and + 80 mV, was also changed by the mutation, from 9 ± 1 $I_{-80}/I_{+80}$ in the WT to 2.9 ± 0.4 $I_{-80}/I_{+80}$ in the mutant. These observations are in agreement with what was previously described by Jenkins *et al.*, 2011. After current stabilisation, 10 µM $L^{-1}$ of AP14145 were applied on the cell transfected with the WT or the mutant protein for 1 - 2 min or until a steady state drug effect was reached (Fig 6a and b).

The experiments showed that, while $rK_{Ca}2.3$ currents recorded from cells transfected with the WT channel were strongly inhibited by application of 10 µM $L^{-1}$ AP14145 (Fig 6a), currents recorded from cells transfected with the mutant $rK_{Ca}.2.3$ were only partially affected by the presence of the compound (Fig 6b). The inhibitory effect of AP14145 was statistically different between the WT and the mutant when analysed as the relative current inhibition after application of AP14145 (95 ± 1 % and 22 ± 6 % inhibition, WT $rK_{Ca}2.3$ vs $rK_{Ca}2.3$ S508T A533V, n = 7 each, Fig 6e).

To ensure that S508 and A533 are important for AP14145 sensitivity, we introduced these amino acids in their homologous positions in the AP14145 insensitive $K_{Ca}3.1$

channel, T250 and V275, respectively. The $K_{Ca}3.1$ T250S V275A mutant was tested using whole cell patch clamp to determine its sensitivity to AP14145. After activation of the channel with 400 nM $L^{-1}$ free [$Ca^{2+}$] intracellular solution and current stabilization, 10 µM $L^{-1}$ AP14145 was applied on the cell. In contrast to the $K_{Ca}3.1$ WT channel (Fig 6c), the mutant $K_{Ca}3.1$ current was inhibited by 92 ± 1 % (n =7, Fig 6d), comparable to the inhibitory effect observed on r$K_{Ca}2.3$.

*AP14145 increases the duration of the atrial effective refractory period in isolated perfused rat hearts*

Excised rat hearts were connected to a retrograde perfusion Langendorff setup to measure the effect of AP14145 on the AERP and discard any $K_{Ca}1.1$ mediated effects.

Once a stable baseline was achieved, the hearts were perfused first with 1 µM $L^{-1}$ of the $K_{Ca}1.1$ inhibitor paxilline. Twenty minutes later, the dose of paxilline was increased to 3 µM $L^{-1}$ for 20 more minutes. Finally, after a 20 minute wash period, 10 µM $L^{-1}$ of AP14145 were perfused into the heart.

Paxilline did not affect the AERP in any of the tested doses, but AP14145 was able to prolong the AERP significantly, from 19 ± 3 ms to 57 ± 12 ms (n = 5, Fig. 7).

*AP14145 increases the duration of the atrial effective refractory period in rats*

To investigate the *in vivo* effects of AP14145, 6 male rats received AP14145 in increasing doses (2.5 mg $kg^{-1}$ and 5 mg $kg^{-1}$) and 6 time matched control rats received corresponding volumes of vehicle (0.5 ml $kg^{-1}$ and 1 ml $kg^{-1}$, respectively).

One minute after injection of 2.5 mg $kg^{-1}$ AP14145 the AERP was significantly increased from 37 ± 2 ms in the time matched control group to 53 ± 6 ms (Fig. 8a). The AERP returned towards baseline values, and five minutes after the injection of 2.5 mg $kg^{-1}$ the AERP was no longer significantly different from that of the time matched controls. One minute after injection of 5 mg $kg^{-1}$ AP14145 the AERP was significantly increased from 31 ± 2 ms in the time matched control group to 58 ± 8 ms (Fig. 8a). Again, the AERP returned towards baseline values, and ten minutes after the injection of 5 mg $kg^{-1}$ the AERP was no longer significantly different from that of the time matched controls.

A third group of rats (n = 6) received a constant rate infusion of 40 mg $kg^{-1}$ $h^{-1}$ over 20 minutes and were monitored for an additional 20 minutes after infusion (Fig 8b). In

these rats the AERP was significantly increased compared to baseline values from 4 minutes after the infusion started (i.e. after a cumulative dose of 2.7 mg $kg^{-1}$). The AERP continued to increase during the rest of the infusion and returned towards baseline values after infusion.

*AP14145 does not impair motor coordination in mice*

A beam walk test was performed in mice in order to assess CNS exposure of $K_{Ca}2$ inhibitors *in vivo*. Three groups of male NMRI mice were used, a vehicle control group (30.5 ± 0.3 g, n = 6), a 10 mg $kg^{-1}$ NS8593 (26 ± 1 g, n = 3) and a 10 mg $kg^{-1}$ AP14145 group (36 ± 5 g, n = 6).

Shortly after the injection of 10 mg $kg^{-1}$ NS8593, all mice showed severe convulsions making them unable to walk on the beam (Fig 9). Therefore, the mice were euthanized by cervical dislocation and the experiment was terminated.

In contrast, when mice were injected with AP14145, no acute effects were observed and the beam walk test was performed 12 minutes after dosing. The mice did not slip or fall from the beam in either of the two tests and no behavioural changes were observed. These observations were not different to the ones from the vehicle control group (Fig 9).

## Discussion

$K_{Ca}2$ channels are inwardly rectifying potassium channels (Köhler et al., 1996) widely distributed in humans, both in the CNS and peripheral tissues (Chen et al., 2004). In the heart, they play an important role in the late repolarization phase of the atria (Li et al., 2009). Moreover, it has been demonstrated that inhibition of $K_{Ca}2$ channels prolongs the AERP (Diness et al., 2010; Skibsbye et al., 2011; Qi et al., 2014; Haugaard et al., 2015). Therefore, the $K_{Ca}2$ channel is considered a promising new target to treat AF. Here we present a new $K_{Ca}2$ inhibitor, AP14145, which could constitute an important tool in rodents, to target and study the inhibition of peripheral $K_{Ca}2.x$ channels *in vivo*.

In initial experiments it was established that AP14145 inhibits $hK_{Ca}2.2$ and $hK_{Ca}2.3$ in an equipotent manner with $IC_{50}$ values of 1.1 ± 0.3 µM $L^{-1}$. To determine the mechanism of inhibition of AP14145, we conducted inside-out patch clamp experiments. Patches were excised from HEK 293 cells stably expressing the $hK_{Ca}2.3$ channel and exposed to a range of intracellular solutions with different free calcium

concentrations. Calcium activation was assessed in the absence and presence of AP14145. The compound significantly increased the $EC_{50}$ of $Ca^{2+}$ from 0.36 ± 0.02 µM $L^{-1}$ to 1.3 ± 0.2 µM $L^{-1}$, thereby shifting the $Ca^{2+}$ activation curve of $K_{Ca}2$ channel activation to higher values. The Hill coefficients were also modified by the presence of AP14145 from 5.2 ± 0.3 to 1.2 ± 0.1 (absence of AP14145 vs. 10 µM $L^{-1}$ AP14145). These results suggest that the drug modifies the channel's calcium sensitivity and acts as a negative allosteric modulator, very similar to the previously reported NS8593. The change of the Hill coefficient may also indicate a loss of calcium cooperativity which may impede calcium binding. Moreover, the inhibitory effect of AP14145 was studied in the presence of the $K_{Ca}2.x$ positive allosteric modulator NS309, which is known to increase the calcium sensitivity of the channel (Strøbæk et al., 2004). In these experiments, AP14145 was able to reverse NS309-mediated $K_{Ca}2.3$ channel activation, suggesting a functional competition between the two compounds and further supporting the negative allosteric mechanism of AP14145.

In the study by Jenkins *et al.* in 2011, the binding site of NS8593, another $K_{Ca}2$ negative allosteric modulator, was found to be located at the inner pore of the channel. This was an interesting finding since the drug had previously been found to decrease calcium sensitivity of the channel and could be speculated to locate the binding site at the C-terminal domain, close to the calmodulin binding domain. Instead, binding interacts with two specific amino acids S507 and A532, located on helixes S5 and S6, respectively. When these two amino acids were mutated to the corresponding residues found on the closely related $K_{Ca}3.1$ channel, which is not inhibited by NS8593, they obtained a $K_{Ca}2.3$ mutant resistant to the effect of the drug, with preserved channel confirmation and calcium sensitivity. In order to find out if AP14145 and NS8593 shared the same binding site, we conducted whole cell patch clamp experiments on transiently transfected HEK cells with $rK_{Ca}2.3$ WT or $rK_{Ca}2.3$ S508T A533V, corresponding to S507 and A532 in the $hK_{Ca}2.3$ channel. While the WT current was strongly inhibited using 10 µM $L^{-1}$ AP14145, the NS8593 resistant mutant was only partially affected by the presence of the drug, suggesting that S508 and A533 are important also for AP14145 inhibition. The loss of AP14145 sensitivity in $rK_{Ca}2.3$ S508T A533V cannot be explained by differences in calcium-activation or channel conformation as these characteristics are preserved in the mutant (Jenkins et al., 2011). AP14145 and NS8593 are structurally close analogues (Fig 1) and these experiments

demonstrate that AP14145 and NS8593 appear to share the same inhibition mechanism as well as some of their binding determinants. Finally, to confirm that S507 and A532 are important for the inhibitory effect of AP14145 on $K_{Ca}2.3$ we introduced these amino acids in their homologous positions on the insensitive $K_{Ca}3.1$ channel. With the addition of these two amino acids, AP14145 sensitivity was fully restored in the $K_{Ca}3.1$ channel (Fig 6), further demonstrating that S507 and A532 are important for AP14145 inhibition. $K_{Ca}2$ channels are widely expressed in the brain, including the cerebellum (Stocker and Pedarzani, 2000), where they contribute to the action potential afterhyperpolarization (Hosy et al., 2011). It has further been demonstrated that inhibition of $K_{Ca}2.2$ channels in cerebellum disturbs the motor output which is revealed as ataxia or convulsion like phenotype especially apparent in the hind legs (Alvina and Khodakhah, 2010). As an indication of CNS exposure and inhibition of central $K_{Ca}2$ channels a beam walk test was performed. The test is designed to assess impaired motor coordination and balance in mice.

Mice injected intravenously with 10 mg $kg^{-1}$ NS8593 immediately showed acute CNS effects in the form of convulsions, and consequently were euthanized. In contrast i.v. injection of 10 mg $kg^{-1}$ AP14145 had no apparent CNS effects, and the mice were able to cross the beam without slipping or falling from the beam, similarly to the vehicle control mice. Importantly, NS8593 plasma protein binding is higher than AP14145 (95.38% vs. 91.35% bound, respectively, Table 1), meaning that a higher amount of AP14145 is freely available in plasma compared to NS8593 when the same dose of both compounds is injected. Moreover, we found that i.v. injection of 2.5 mg $kg^{-1}$ AP14145 significantly increases the atrial refractoriness in rats within 1 min of injection, suggesting that 10 mg $kg^{-1}$ is sufficient to peripheral $K_{Ca}2$ target engagement.

A possible explanation for the apparent difference in CNS penetration of the two compounds lies in their structure (Fig 1) and physicochemical properties (Table 1). In particular, AP14145 contains a carboxamide moiety on the bicyclic benzimidazole ring, a chemical moiety that adds polarity to the molecule and is known to be a common substrate for P-glycoprotein transporter mediated efflux. The calculated polar surface area (PSA) of AP14145 is 70, which is significantly higher than NS8593 (Table 1), indicating a lower likelihood of penetrating the blood-brain barrier. It can thus be hypothesised that the structural features in AP14145 make the compound less likely to penetrate to induce CNS mediated convulsions when compared to NS8593. Although

this difference in profile could in principle be caused by differences in the pharmacokinetic profile of the two compounds, this seems an unlikely explanation, since, as has been shown in Diness et al. (2010), 5 mg $kg^{-1}$ of NS8593 cause similar increases of the AERP in rats when compared to the effect of 5 mg $kg^{-1}$ of AP14145 (Fig 8a).

High concentrations of AP14145 (10 µM L-1) significantly inhibited the $K_{Ca}1.1$ channel. However, as paxilline, which is a well-known specific inhibitor of $K_{Ca}1.1$ channels (Nardi and Olesen, 2008), did not have any effect on the atrial refractoriness of isolated perfused rat hearts, we conclude that the inhibition of $K_{Ca}1.1$ by AP14145 does not contribute to the AERP prolonging effects of AP14145. This is in accordance with studies demonstrating the lack of $K_{Ca}1.1$ channels and currents in the plasma membrane of cardiomyocytes (Bautista et al., 2009; Singh et al., 2013).

The apparent reduced CNS exposure of the drug makes AP14145 a unique and useful new tool compound that allows the study of peripheral $K_{Ca}2$ inhibition without apparently interfering with CNS function in awake rodents. This might help further development and understanding of the cardiac and endothelial role of $K_{Ca}2$ in a number of physiological and pathological settings.

## Conclusions

In this work we present the novel $K_{Ca}2$ negative gating modulator AP14145. This new drug inhibits both the $hK_{Ca}2.2$ and $hK_{Ca}2.3$ with equal potency ($IC_{50}$ = 1.1 ± 0.3 µM $L^{-1}$ with 400 nM $L^{-1}$ intracellular $Ca^{2+}$) by decreasing the calcium sensitivity of the channel. The inhibitory effect of AP14145 effect is strongly dependent on two amino acids, S508 and A533 in the $rK_{Ca}2.3$, located in the inner pore of the channel. *In vivo,* AP14145 significantly increases the atrial refractoriness in rats shortly after a 2.5 mg $kg^{-1}$ or 5.0 mg $kg^{-1}$ bolus injection. In contrast to NS8593, a dose of 10 mg $kg^{-1}$ of AP14145 did not trigger any apparent acute CNS mediated effects in mice, suggesting that the compound does not penetrate the blood brain barrier to the same degree as NS8593 in rodents. This key difference could for the first time allow for the use of a $K_{Ca}2$ negative modulator *in vivo* without interfering with CNS function. We expect this feature might help further development and understanding of the cardiac and endothelial role of $K_{Ca}2$ channels.

## Author contributions

*Rafel Simó-Vicens:* conception and design of the study, data acquisition (electrophysiology and molecular biology) and analysis, drafting and critical revision of the work.

*Jeppe E. Kirchhoff:* acquisition of data (closed chest recordings), data analysis, drafting and critical revision of the work.

*Lea Abildgaard Jensen:* acquisition of data (beam walk test and perfused heart preparation), data analysis, drafting and critical revision of the work.

*Bernardo Dolce:* data acquisition (electrophysiology and molecular biology) and analysis.

*Tobias Speerschneider:* acquisition of data (closed chest recordings), data analysis, drafting and critical revision of the work.

*Ulrik S. Sørensen:* conception and design of AP14145, conception and design of the study, drafting and critical revision of the work.

*Morten Grunnet:* conception and design of the study, critical revision of the work.

*Jonas G. Diness:* conception and design of the study, data analysis, drafting and critical revision of the work.

*Bo H. Bentzen:* conception and design of the study, drafting and critical revision of the work.

## Acknowledgements

The study was supported by Innovation Fund Denmark, the Carlsberg Foundation, and the European Union's Horizon 2020 research and innovation programme under the Marie Skłodowska-Curie grant agreement No. 675351. We would also like to thank Dorte Strøbæk for kindly donating the $hK_{Ca}3.1$ T250S V275A mutant.

## Conflicts of interest statement

All authors of this study are or have been employed by Acesion Pharma.

## References


Adelman, J.P. (2016). SK channels and calmodulin. Channels *10*: 1–6.

Alexander, S., Catterall, W., Kelly, E., Marrion, N., Peters, J., Benson, H., et al. (2015). The Concise Guide to PHARMACOLOGY 2015/16: Voltage-gated ion channels. Br J Pharmacol. *172*: 5904–5941.

Alvina, K., and Khodakhah, K. (2010). KCa channels as therapeutic targets in episodic ataxia type-2. J Neurosci *30*: 7249–7257.

Bautista, L., Castro, M.J., López-Barneo, J., and Castellano, A. (2009). Hypoxia inducible factor-2α stabilization and maxi-K+ channel β1-subunit gene repression by hypoxia in cardiac myocytes: Role in preconditioning. Circ. Res. *104*: 1364–1372.

Brooks, S.P., and Dunnett, S.B. (2009). Tests to assess motor phenotype in mice: a user's guide. Nat. Rev. Neurosci. *10*: 519–29.

Chen, M.X., Gorman, S.A., Benson, B., Singh, K., Hieble, J.P., Michel, M.C., et al. (2004). Small and intermediate conductance Ca2+-activated K+ channels confer distinctive patterns of distribution in human tissues and differential cellular localisation in the colon and corpus cavernosum. Naunyn. Schmiedebergs. Arch. Pharmacol. *369*: 602–615.

Christophersen, I.E., Rienstra, M., Roselli, C., Yin, X., Geelhoed, B., Barnard, J., et al. (2017). Large-scale analyses of common and rare variants identify 12 new loci associated with atrial fibrillation. Nat. Genet. *49*:.

Diness, J.G., Bentzen, B.H., Sørensen, U.S., and Grunnet, M. (2015). Role of Calcium-activated Potassium Channels in Atrial Fibrillation Pathophysiology and Therapy. J. Cardiovasc. Pharmacol. *66*: 441–8.

Diness, J.G., Sørensen, U.S., Nissen, J.D., Al-Shahib, B., Jespersen, T., Grunnet, M., et al. (2010). Inhibition of small-conductance ca2+-activated k+ channels terminates and protects against atrial fibrillation. Circ. Arrhythmia Electrophysiol. *3*: 380–390.

Ellinor, P.T., Lunetta, K.L., Glazer, N.L., Pfeufer, A., Alonso, A., Chung, M.K., et al.

(2010). Common variants in KCNN3 are associated with lone atrial fibrillation. Nat. Genet. *42*: 240–244.

Habermann, E. (1984). Apamin. Pharmac. Ther. *25*: 255–270.

Haugaard, M.M., Hesselkilde, E.Z., Pehrson, S., Carstensen, H., Flethøj, M., Præstegaard, K.F., et al. (2015). Pharmacologic inhibition of small-conductance calcium-activated potassium (SK) channels by NS8593 reveals atrial antiarrhythmic potential in horses. Hear. Rhythm *12*: 825–835.

Hosy, E., Piochon, C., Teuling, E., Rinaldo, L., Hansel, C., and Hansel, C. (2011). SK2 channel expression and function in cerebellar Purkinje cells. J Physiol J. Physiol. S *58914*: 3433–3440.

Jenkins, D.P., Strobaek, D., Hougaard, C., Jensen, M.L., Hummel, R., Sorensen, U.S., et al. (2011). Negative gating modulation by (R)-N-(benzimidazol-2-yl)-1,2,3,4-tetrahydro-1-naphthylamine (NS8593) depends on residues in the inner pore vestibule: pharmacological evidence of deep-pore gating of K(Ca)2 channels. Mol.Pharmacol. *79*: 899–909.

Köhler, M., Hirschberg, B., Bond, C.T., Kinzie, J.M., Marrion, N. V, Maylie, J., et al. (1996). Small-Conductance, Calcium-Activated Potassium Channels from Mammalian Brain. Science (80-. ). *273*: 1709–1714.

Lam, J., Coleman, N., Lourdes A. Garing, A., and Wulff, H. (2013). The Therapeutic Potential of Small-Conductance KCa2 Channels in Neurodegeneratve and Psychiatric Diseases. *17*: 1203–1220.

Li, N., Timofeyev, V., Tuteja, D., Xu, D., Lu, L., Zhang, Q., et al. (2009). Ablation of a Ca2+-activated K+ channel (SK2 channel) results in action potential prolongation in atrial myocytes and atrial fibrillation. J. Physiol. *587*: 1087–100.

Milkau, M., Köhler, R., and Wit, C. de (2010). Crucial importance of the endothelial K+ channel SK3 and connexin40 in arteriolar dilations during skeletal muscle contraction. FASEB J. *24*: 3572–3579.

Nardi, A., and Olesen, S.-P. (2008). BK channel modulators: a comprehensive overview. Curr. Med. Chem. *15*: 1126–46.

Nattel, S. (2002). New ideas about atrial fibrillation 50 years on. Nature *415*: 219–26.

Pedarzani, P., McCutcheon, J.E., Rogge, G., Jensen, B.S., Christophersen, P., Hougaard, C., et al. (2005). Specific enhancement of SK channel activity selectively potentiates the afterhyperpolarizing current IAHP and modulates the firing properties of hippocampal pyramidal neurons. J. Biol. Chem. *280*: 41404–41411.

Qi, X.Y., Diness, J.G., Brundel, B.J.J.M., Zhou, X.B., Naud, P., Wu, C.T., et al. (2014). Role of small-conductance calcium-activated potassium channels in atrial electrophysiology and fibrillation in the dog. Circulation *129*: 430–440.

Schmitt, N., Grunnet, M., and Olesen, S.-P. (2014). Cardiac potassium channel subtypes: new roles in repolarization and arrhythmia. Physiol. Rev. *94*: 609–53.

Singh, H., Lu, R., Bopassa, J.C., Meredith, A.L., Stefani, E., and Toro, L. (2013). mitoBKCa is encoded by the Kcnma1 gene, and a splicing sequence defines its mitochondrial location. Proc. Natl. Acad. Sci. U. S. A. *110*: 10836–10841.

Skibsbye, L., Diness, J.G., Sørensen, U.S., Hansen, R.S., and Grunnet, M. (2011). The duration of pacing-induced atrial fibrillation is reduced in vivo by inhibition of small conductance Ca(2+)-activated K(+) channels. J. Cardiovasc. Pharmacol. *57*: 672–681.

Southan, C., Sharman, J.L., Benson, H.E., Faccenda, E., Pawson, A.J., Alexander, S.P.H., et al. (2016). The IUPHAR/BPS Guide to PHARMACOLOGY in 2016: Towards curated quantitative interactions between 1300 protein targets and 6000 ligands. Nucleic Acids Res. *44*: D1054–D1068.

Stocker, M., and Pedarzani, P. (2000). Differential distribution of three Ca(2+)-activated K(+) channel subunits, SK1, SK2, and SK3, in the adult rat central nervous system. Mol. Cell. Neurosci. *15*: 476–493.

Strøbæk, D., Hougaard, C., Johansen, T.H., Sørensen, U.S., Nielsen, E.O., Nielsen, K.S., et al. (2006). Inhibitory gating modulation of small conductance Ca2+-activated K+ channels by the synthetic compound (R)-N-(benzimidazol-2-yl)-1,2,3,4-tetrahydro-1-naphtylamine (NS8593) reduces afterhyperpolarizing current in hippocampal CA1 neurons. Mol. Pharmacol. *70*: 1771–1782.

Strøbæk, D., Teuber, L., Jørgensen, T.D., Ahring, P.K., Kjær, K., Hansen, R.S., et al. (2004). Activation of human IK and SK Ca 2+-activated K + channels by NS309 (6,7-dichloro-1H-indole-2,3-dione 3-oxime). Biochim. Biophys. Acta - Biomembr. *1665*: 1–5.

Sørensen, U.S., Strøbæk, D., Christophersen, P., Hougaard, C., Jensen, M.L., Nielsen, E., et al. (2008). Synthesis and structure-activity relationship studies of 2-(N-substituted)-aminobenzimidazoles as potent negative gating modulators of small conductance Ca2+-activated K+ channels. J. Med. Chem. *51*: 7625–7634.

Waks, J.W., and Zimetbaum, P. (2017). Antiarrhythmic Drug Therapy for Rhythm Control in Atrial Fibrillation. J. Cardiovasc. Pharmacol. Ther. *22*: 3–19.

Wulff, H., Kolski-Andreaco, A., Sankaranarayanan, A., Sabatier, J.-M., and Shakkottai, V. (2007). Modulators of small- and intermediate-conductance calcium-activated potassium channels and their therapeutic indications. Curr Med Chem *14*: 1437–1457.

Zoni-Berisso, M., Lercari, F., Carazza, T., and Domenicucci, S. (2014). Epidemiology of atrial fibrillation: European perspective. Clin. Epidemiol. *6*: 213.

## Supporting information

None supplied.

## Figures and figure legends

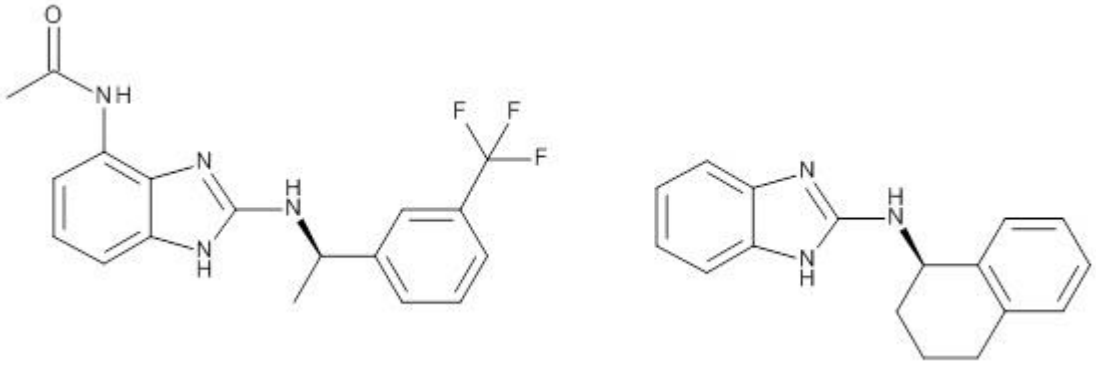


Fig. 1. Chemical structures of AP14145 (left) and NS8593 (right).

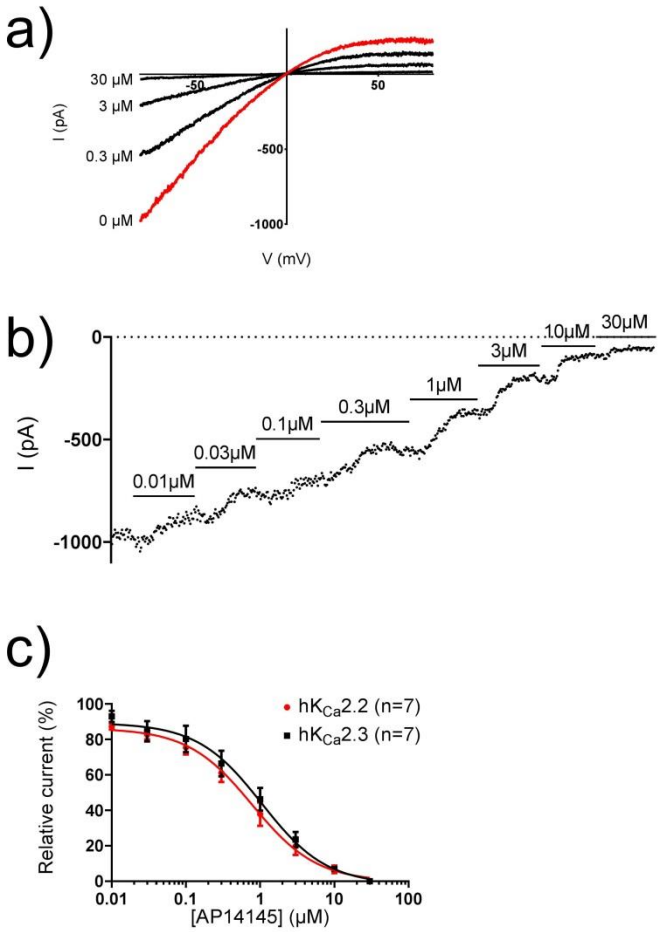


694

695 Fig. 2. a) Representative current-voltage recordings of the inhibition of $hK_{Ca}2.3$ by
696 increasing concentrations of the drug AP14145 and b) its current-time plot obtained by
697 inside-out patch clamp on HEK cells stably expressing the channel. c) Inhibition curves
698 of AP14145 on both the $hK_{Ca}2.2$ (n = 7) and $hK_{Ca}2.3$ ( n = 7) channel.

699

700

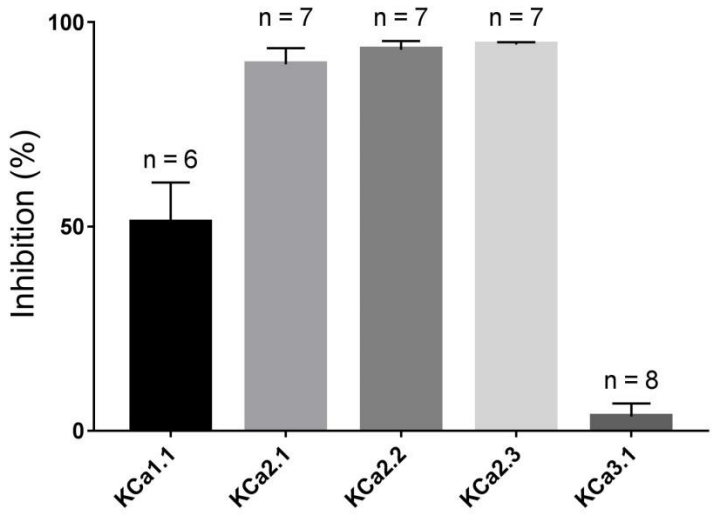


Fig. 3. Inhibitory effect of 10 µM $L^{-1}$ AP14145 on $K_{Ca}1.1$, $K_{Ca}2.1$, $K_{Ca}2.2$, $K_{Ca}2.3$ and $K_{Ca}3.1$ channels. All measurements were obtained by whole cell patch clamp except $K_{Ca}2.2$, which were obtained by inside-out patch clamp.

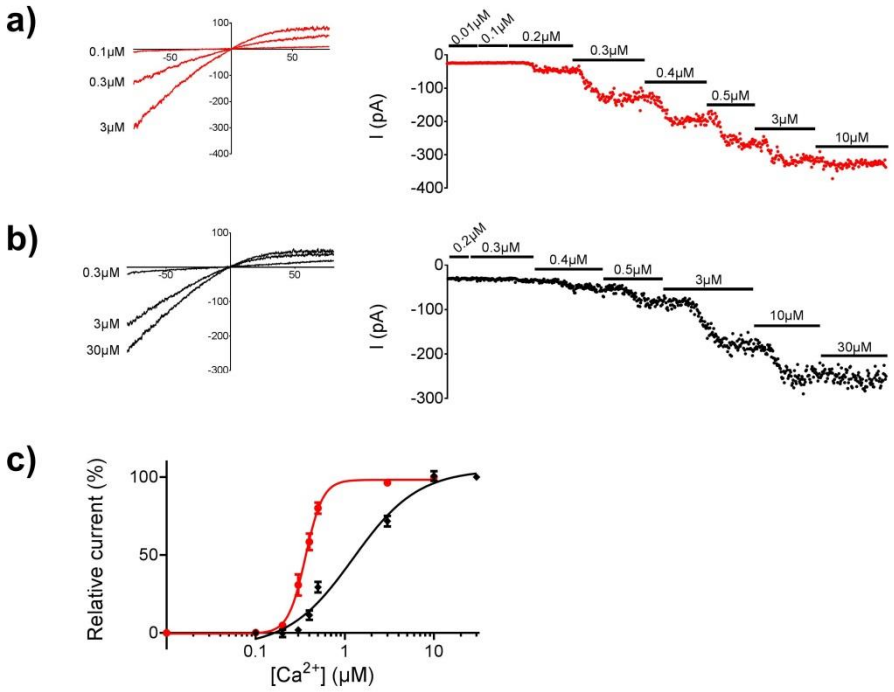


Fig. 4. Representative current-voltage plots (left) and their corresponding current-time plots (right) of h$K_{Ca}2.3$ calcium activation a) in the absence of AP14145 and b) in the presence of 10 µM $L^{-1}$ AP14145. c) Calcium activation curves for the h$K_{Ca}2.3$ channel in the absence of AP14145 (red curve, n = 9) and in the presence of 10 µM $L^{-1}$ AP14145 (black curve, n = 7).

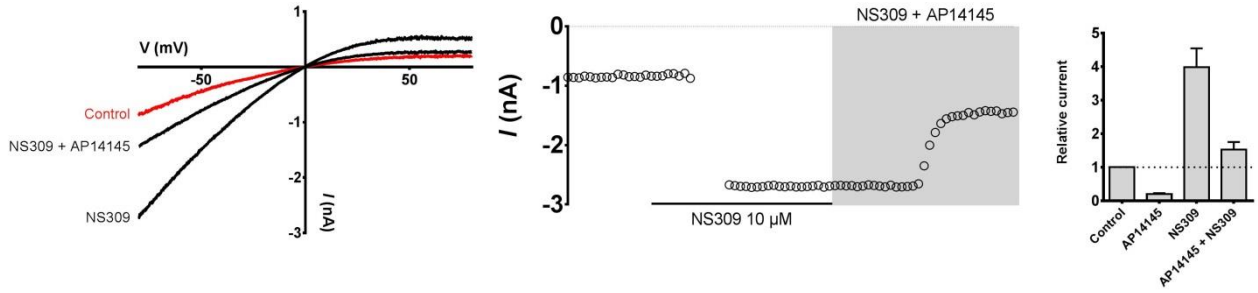


711

712 Fig. 5. Representative current-voltage plot (left) and its corresponding current-time plot
713 (centre) of the effect of 10 µM $L^{-1}$ NS309 in the absence and in the presence of 10 µM
714 $L^{-1}$ AP14145 on excised $hK_{Ca}2.3$ patches. On the right, bar graph comparing the effects
715 of 10 µM $L^{-1}$ AP14145 (n = 7), 10 µM $L^{-1}$ NS309 (n = 7), and 10 µM $L^{-1}$ AP14145 + 10
716 µM $L^{-1}$ NS309 (n = 7) on excised $hK_{Ca}2.3$ patches.

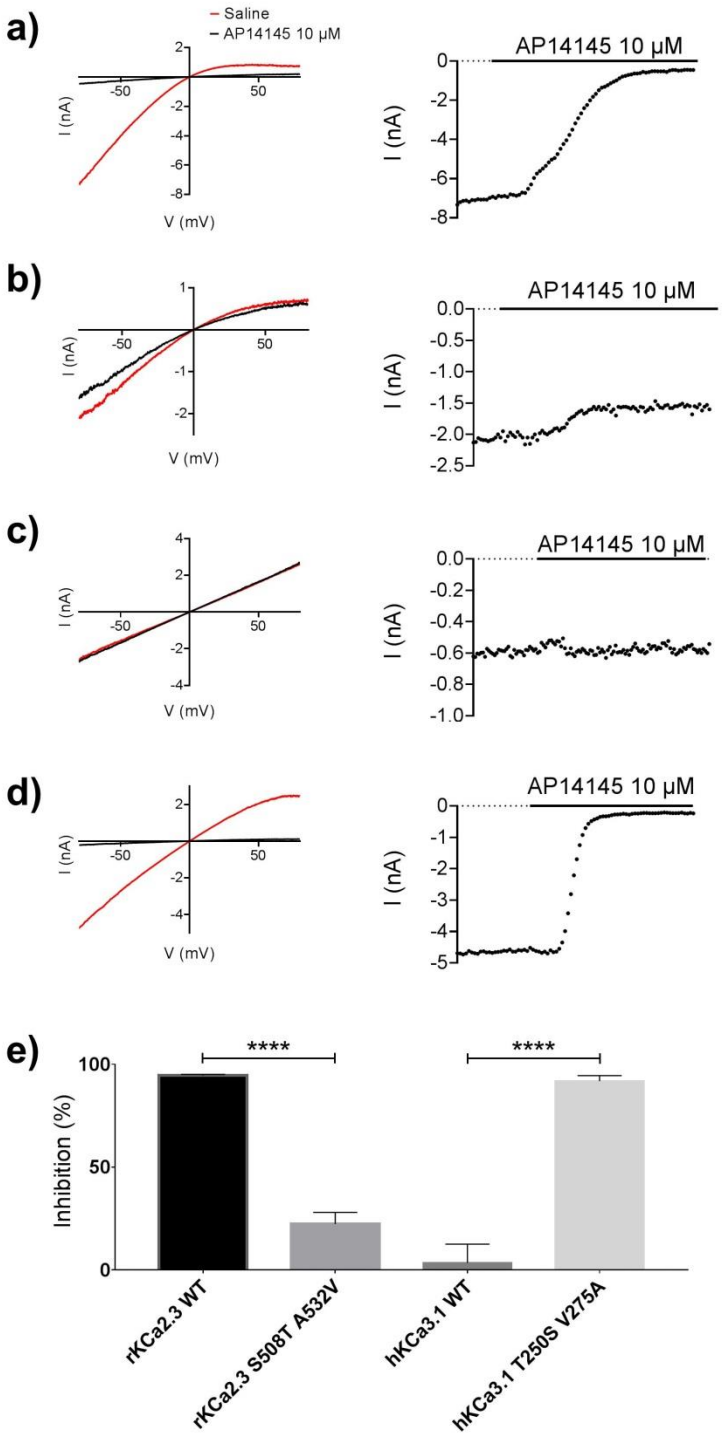


Fig. 6. Representative current-voltage plots (left) and current-time plots (right) depicting the effect of AP14145 10 µM $L^{-1}$ on HEK cells transiently transfected with a) $rK_{Ca}2.3$ WT, b) $rK_{Ca}2.3$ S508T A533V, c) $hK_{Ca}3.1$ WT and d) $hK_{Ca}3.1$ T250S V275A recorded using whole cell patch clamp. e) Bar graph comparing the inhibitory effect of 10 µM $L^{-1}$ AP14145 on $rK_{Ca}2.3$ WT (n = 7), $rK_{Ca}2.3$ S508T A533V (n = 7), $hK_{Ca}3.1$ WT channel (n = 8) and $hK_{Ca}3.1$ T250S V275A (n = 7).

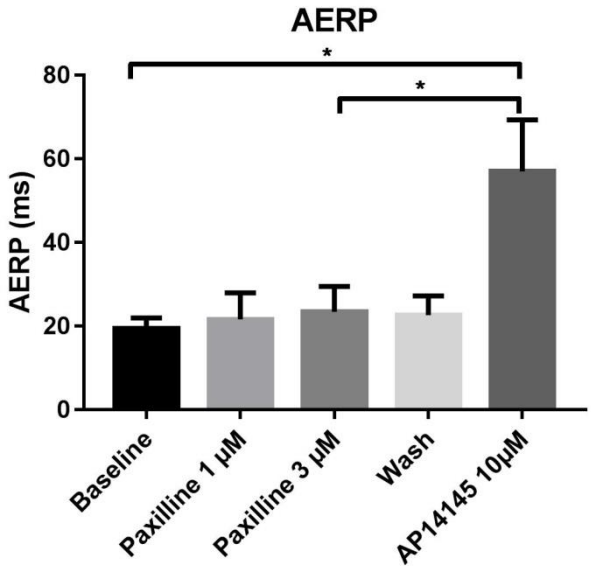


Fig 7. Effect of 1 µM $L^{-1}$ and 3 µM $L^{-1}$ of the $K_{Ca}1.1$ inhibitor paxilline and 10 µM $L^{-1}$ AP14145 on the AERP of isolated perfused rat hearts (n = 5).

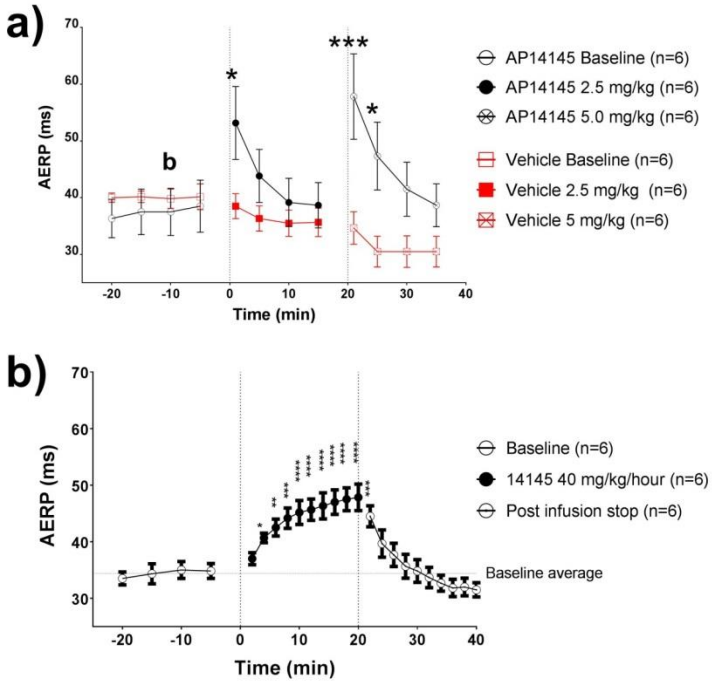


Fig. 8. Effects on AERP in closed chest in vivo rats: a) Bolus doses of 2.5 mg $kg^{-1}$ and 5 mg $kg^{-1}$ AP14145 significantly increased the AERP compared to time matched controls receiving corresponding volumes of vehicle. b) AP14145 given as a constant rate infusion of 40 mg $kg^{-1}$ $h^{-1}$ over 20 minutes increased AERP compared to the baseline average and returned towards baseline values post-infusion.

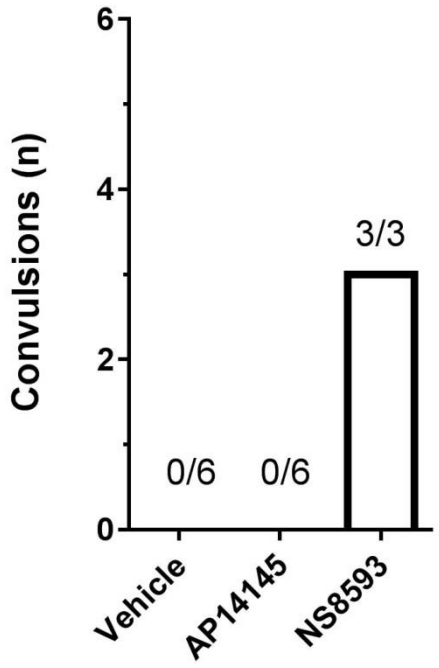


733

734 Fig. 9. Bar graph depicting the amount of convulsions triggered by the administration of
735 the vehicle, 10 mg kg $^{-1}$ AP14145 and 10 mg kg $^{-1}$ NS8593.

736

737 Table 1. Calculated physicochemical properties and plasma protein binding (PPB) of
738 NS8593 and AP14145.

| | **log D (pH 7.4)** | **log P** | **PSA (Å$^2$)** | **PPB (% bound)** |
|---|---|---|---|---|
| **NS8593** | 4.0 | 4.1 | 41 | 95.38 |
| **AP14145** | 3.6 | 3.7 | 70 | 91.35 |

739

740

741